

# Comprehensive and Systematic Analysis of the Immunocompatibility of Polyelectrolyte Capsules

Mikhail V. Zyuzin,<sup>†</sup> Paula Díez,<sup>‡,§</sup> Meir Goldsmith,<sup>||</sup> Susana Carregal-Romero,<sup>†,⊥</sup> Cristina Teodosio,<sup>‡</sup> Joanna Rejman,<sup>†</sup> Neus Feliu,<sup>†</sup> Alberto Escudero,<sup>†,#</sup> María Jesús Almendral,<sup>¶</sup> Uwe Linne,<sup>○</sup> Dan Peer,<sup>\*,||</sup> Manuel Fuentes,<sup>\*,‡,§</sup> and Wolfgang J. Parak<sup>\*,†,⊥,||</sup>

<sup>†</sup>Fachbereich Physik and <sup>○</sup>Fachbereich Chemie, Philipps Universität Marburg, 35037 Marburg, Germany

<sup>‡</sup>Department of Medicine and General Cytometry Service-Nucleus and <sup>§</sup>Proteomics Unit, Cancer Research Centre (IBMCC/CSIC/USAL/IBSAL), 37007 Salamanca, Spain

<sup>||</sup>Laboratory of PrecisionNanoMedicine, Department of Cell Research and Immunology, George S. Wise Faculty of Life Sciences, Department of Materials Science and Engineering, The Iby and Aladar Fleischman Faculty of Engineering, Center for Nanoscience and Nanotechnology, Tel Aviv University, Tel Aviv 6997801, Israel

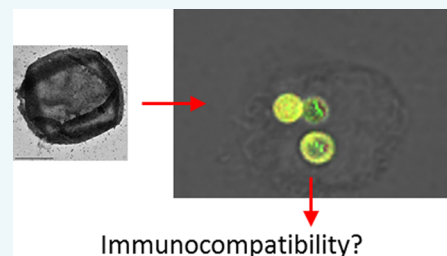
<sup>⊥</sup>CIC biomaGUNE, Paseo de Miramón 182, 20014 Donostia – San Sebastián, Spain

<sup>#</sup>Instituto de Ciencia de Materiales de Sevilla, CSIC – Universidad de Sevilla, C. Américo Vespucio 49, E-41092, Sevilla, Spain

<sup>¶</sup>Department of Analytical Chemistry, Nutrition and Food Science, Faculty of Chemistry, University of Salamanca, 37008 Salamanca, Spain

## Supporting Information

**ABSTRACT:** The immunocompatibility of polyelectrolyte capsules synthesized by layer-by-layer deposition has been investigated. Capsules of different architecture and composed of either non-degradable or biodegradable polymers, with either positively or negatively charged outer surface, and with micrometer size, have been used, and the capsule uptake by different cell lines has been studied and quantified. Immunocompatibility studies were performed with peripheral blood mononuclear cells (PBMCs). Data demonstrate that incubation with capsules, at concentrations relevant for practical applications, did not result in a reduced viability of cells, as it did not show an increased apoptosis. Presence of capsules also did not result in an increased expression of TNF- $\alpha$ , as detected with antibody staining, as well as at mRNA level. It also did not result in increased expression of IL-6, as detected at mRNA level. These results indicate that the polyelectrolyte capsules used in this study are immunocompatible.



## INTRODUCTION

Polyelectrolyte capsules assembled by the layer-by-layer strategy<sup>1,2</sup> are a universal carrier platform,<sup>3</sup> and they can integrate many functionalities in the cavity as well as in the capsule walls.<sup>4–8</sup> Capsules have been demonstrated to be versatile tools for controlled delivery of proteins, enzymes, and other molecules of biomedical interest,<sup>9</sup> and they have also been used for sensing applications,<sup>10</sup> as reported in many studies based on different cell lines. Capsules can be synthesized from a large range of materials, allowing, for example, tuning of degradability, by using different-sized template core diameters ranging from a few nanometers up to micrometers, and production can be scaled up.<sup>11</sup> However, in vivo applications, which would be the first step toward future clinical use, have so far only been reported in a limited amount of studies. These in vivo works range from fundamental studies about the uptake of capsules;<sup>12</sup> delivery of pharmaceutical agents such as antibiotics,<sup>13,14</sup> antigens/vaccines,<sup>15–17</sup> growth factors,<sup>18</sup> or chemotherapeutics;<sup>19,20</sup> light-triggered release of anticancer drugs<sup>21</sup> or signaling molecules;<sup>22</sup> photothermal heating;<sup>23</sup>

combinations of both;<sup>24</sup> and imaging.<sup>25</sup> While capsules for intravenous administration should be small enough to avoid blockade of blood vessels, size is less relevant, for example, in vaccination.<sup>15,26</sup> The size of polyelectrolyte capsules can be tuned by the size of their template core and can be in the range of a few tens of nanometers up to tens of micrometers. For in vivo application, biocompatibility of the capsules is mandatory. However, so far most studies in this direction have been performed in vitro with cell lines. Cell lines, as primary cultures,<sup>27</sup> endocytose capsules,<sup>28</sup> which, if they are composed of biodegradable polymers, may be degraded inside lysosomes.<sup>29,30</sup> Dependence of this uptake regarding charge,<sup>31</sup> shape,<sup>32</sup> stiffness,<sup>33</sup> and formation of a protein corona<sup>31,34</sup> has been investigated. It has been reported that positively charged, elongated, and soft capsules are more rapidly internalized than negatively charged, flat, and stiff capsules. In cases where the

Received: November 10, 2016

Revised: December 23, 2016

Published: January 2, 2017

density of capsules to which cells are exposed is as high as that of sediment on top of cells, reduction in cell viability has been observed.<sup>35</sup> In general, capsules have been reported to be potentially toxic in cases where toxic compounds are integrated.<sup>35,36</sup> However, if their shell is composed of nontoxic polymers, in particular, biocompatible polymers, standard viability test shows that the exposure of capsules to cells at densities realistic for applications does not exhibit acute cell damage.<sup>36–44</sup> Capsules composed of multiple polyelectrolyte layers may induce less toxicity than the individual polyelectrolytes.<sup>45</sup> Highly cationic polyelectrolytes, which are in general considered toxic, are upon the formation of capsules partly complexed by anionic polyelectrolytes<sup>46</sup> (even when they form the outer surface), and this has been considered a reason for the low toxicity of such positively charged capsules. However, most of the toxicity studies reported in the literature have been performed on the basis of simple viability assays. In vivo applications demand a more sophisticated test, such as assays on the immunocompatibility of capsules.<sup>47</sup> This report aims to shed more light on the immunocompatibility of capsules. Assays were carried out with peripheral blood mononuclear cells (PBMCs), for which, upon exposure to capsules, their cytokine expression was analyzed with antibody staining as well as at the mRNA level.

## RESULTS AND DISCUSSION

**Capsule Preparation and Characterization.** Eight different capsule samples were prepared. They were composed of non-degradable or biodegradable polyelectrolytes, negatively or positively charged, and with or without integrated semianaphtharhodafuor dye (SNARF-1). The diameter of all capsules was around 3  $\mu\text{m}$ , as determined by bright field microscopy (cf. Supporting Information Figure SI–I.5.1 and Table SI–I.5.1). The integration of SNARF-1 into the cavity of the capsules did not significantly change the capsule diameter. The presence of SNARF-1 could be verified by fluorescence microscopy due to the change of fluorescence color from yellow to red upon increasing the pH from acidic to alkaline condition (cf. Supporting Information Figures SI–I.5.3 to SI–I.5.6).<sup>48</sup> Transmission electron microscopy (TEM) images showed the typical form of capsules collapsed under vacuum, which indicated that the template cores were successfully dissolved (cf. Figure SI–I.5.2). A sketch of the capsules and selected images are presented in Figure 1. For further details about the

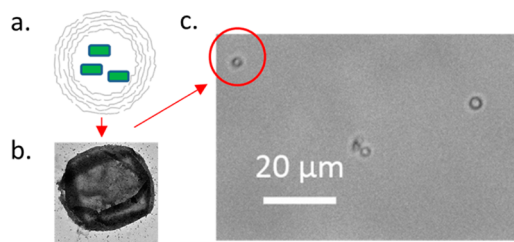


**Figure 1.** (a) Sketch of one polyelectrolyte capsule showing the layer-by-layer assembly of the polyelectrolyte wall (gray) and the embedded fluorophores (green). (b) TEM of one capsule of (DEXS/PARG)<sub>4</sub>DEXS geometry; the scale bar indicates 1  $\mu\text{m}$ . (c) Optical bright field image of three capsules of (DEXS/PARG)<sub>4</sub>DEXS geometry. From these images the diameter was determined to be  $3.02 \pm 0.24 \mu\text{m}$ .

characterization we refer to the Supporting Information and to previous publications.<sup>29</sup> The pattern of adsorbed proteins to the capsules (without integrated SNARF-1) was similar

(cf. Table SI–II.1.1). The most abundant protein detected was alpha-2-HS-glycoprotein. We speculated that this protein, known to form complexes with calcium and phosphate,<sup>49,50</sup> may bind to residual fragments of CaCO<sub>3</sub> template cores, which have not entirely dissolved. While we clearly observe the formation of a protein corona around the capsules, the differences found within the types of capsules are not that significant, as one would expect the different protein coronas to impregnate different capsule interactions with cells. The full data sets corresponding to the characterization of protein corona are shown in the Supporting Information.

### Quantitative Uptake of Capsules by Different Cells.

Using SNARF-1 as pH indicator inside the capsules, internalized capsules (yellow fluorescence due to acidic pH in lysosomes) could be clearly distinguished from extracellular capsules (red fluorescence in neutral cell medium) and thus the number of internalized capsules per cells could be estimated quantitatively (cf. Figures SI–III.2.1, SI–III.2.2, and Table SI–III.3).<sup>28</sup> The number of internalized capsules per cell was visualized in the form of histograms (cf. Figures SI–III.3.1 to SI–III.3.12), and cumulative distribution functions derived from the histograms (cf. Figure 2). It is well-known that under serum containing conditions differences in the uptake behavior of capsules due to different physicochemical parameters such as polarity of the surface charge are less pronounced as compared to serum-free conditions.<sup>31</sup> This is ascribed to the formation of the protein corona, which “shields” the original surface chemistry. From the uptake study carried out here in serum-containing media, several general tendencies could be observed, and due to the variation of several key parameters (such as cell line, incubation time, number of added capsules per cell, degradability of the capsule shell, polarity of the capsule shell, among others), a comprehensive data set could be obtained (cf. Table SI–III.4.1 and Figures SI–III.4.2 to SI–III.4.6). First, in basically all cases the addition of 10 capsules per cell as compared to 5 capsules per cell resulted in more internalized capsules (cf. Figure 2a). This showed that under these conditions of uptake, saturation has not been reached. Second, incubation of cells with capsules for 24 h instead of 12 h resulted in more internalized capsules (cf. Figure 2b). The only exceptions we found were related to some of the biodegradable capsules. However, as those upon degradation lose their integrity and shape the most likely explanation is that some of the degraded capsules were not identified and thus are missing in the number of counted capsules per cell. Third, surprisingly the differences in charge-dependent uptake are moderate. Only in the case of A549 cells was a general enhanced uptake for positively versus negatively charged capsules found, whereas for the other two cell types no clear tendency was found (cf. Figure 2c). This is likely due to the formation of the protein corona, which tends to cover changes in the original surface chemistry. Fourth, for A549 cells more non-degradable than degradable capsules were internalized, in contrast to the case of MDMs, in which more degradable than non-degradable capsules were found in cells. In the case of HeLa cells there was no tendency to be observed (cf. Figure 2d). The raw data of this analysis are provided in the Supporting Information. The data demonstrate that uptake behavior for the different capsule types in serum-containing media is relatively similar.

**Simultaneous Multiparametric Flow Cytometry Analysis of Viability and Immune Response to Different Stimuli.** All the polyelectrolyte capsules were incubated with hematological cell lines as models and peripheral blood

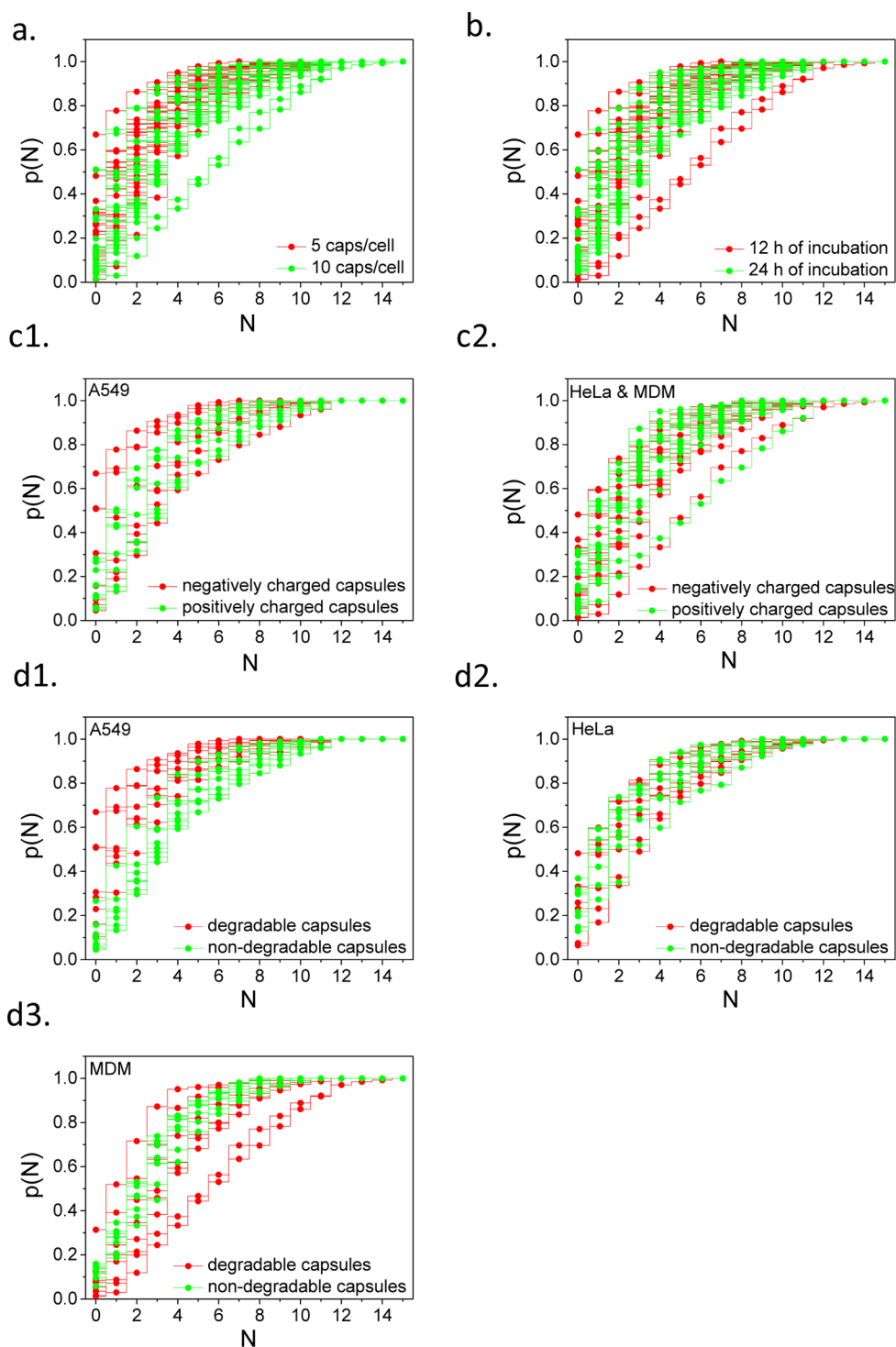


**Figure 2.** Cumulative probability plots  $p(N)$  for the different experiments obtained for the following parameters: cell line, incubation time, number of added capsules per cell, degradability of the capsule shell, and polarity of the capsule shell. In each figure, only one parameter is highlighted by color, whereas the traces for all the different parameters are shown in the same color. (a) 5 and 10 capsules added per cell plotted in red and green, respectively. (b) 12 and 24 h incubation time plotted in red and green, respectively. (c) Negatively and positively charged capsules plotted in red and green, respectively, for (c1) A549 cells and (c2) for HeLa and MDM cells. (d) Degradable versus nondegradable capsules plotted in red and green, respectively, for (d1) A549 cells, (d2) HeLa cells, and (d3) MDM cells.

mononuclear cells (PBMCs). In all cases the phagocytic capacity, cytokine activation, and cytotoxicity were simultaneously evaluated for all polyelectrolyte capsules by flow cytometry in one single assay.

To evaluate the effect of exposure of hematopoietic cells to the capsules, an MTT (3-(4,5-dimethylthiazol-2-yl)-2,5-diphenyl

tetrazolium bromide) assay was performed in two cell lines, Jurkat and dTHP-1, used as models of T-lymphocytes and monocytes, respectively (cf. Figure SI-IV.6). The obtained results (cf. Figure 3) showed that capsules were highly biocompatible, as the average percentage of viable cells in all cases was above 90% for both cell lines (more detailed information is

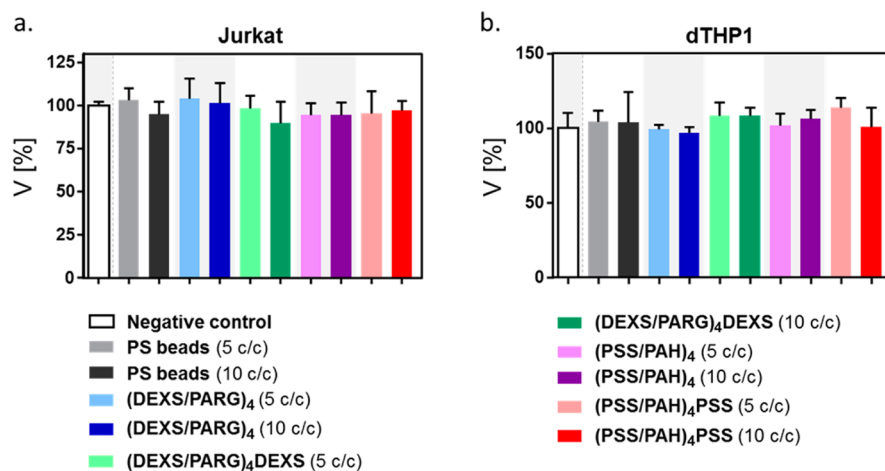


**Figure 3.** Effect of polyelectrolyte capsules on cell viability ( $V$  [%]) of (a) Jurkat and (b) dTHP-1 cells, PS microsphere capsules or polyelectrolyte capsules, during 12 h, as determined by MTT assay. Data are presented as mean values  $\pm$  standard deviation (SD) of 3 replicates. PS = polystyrene latex, c/c = capsules per cell.

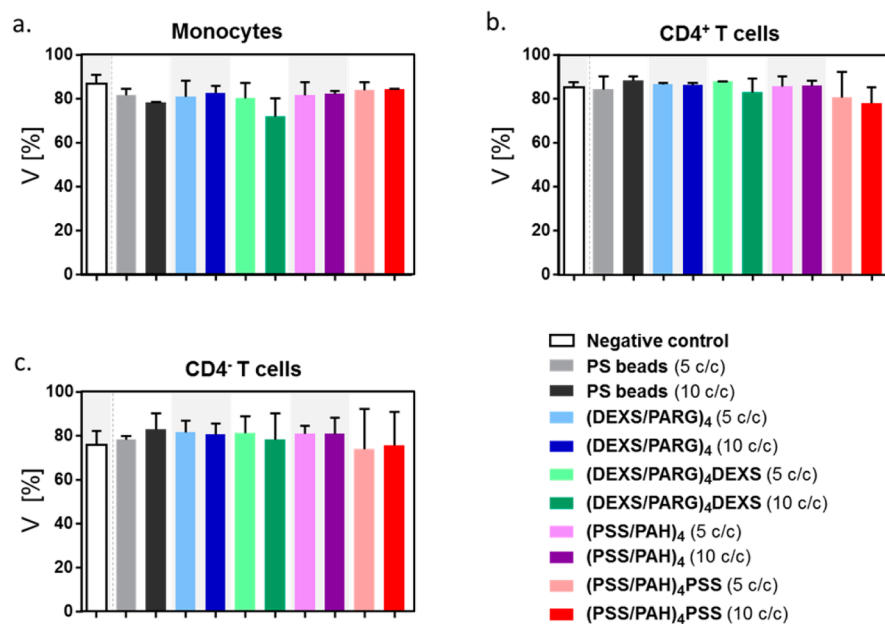


**Figure 4.** Effect of polyelectrolyte capsules on cell viability of ( $V$  [%]) of (a) monocytes, (b) CD4<sup>+</sup>, and (c) CD4<sup>-</sup> T cells. PBMCs were incubated without (“Negative control”) PS microspheres or polyelectrolyte capsules, during 4 h, as determined by the lack of expression of annexin V. Values represent the mean  $\pm$  SD of two biological replicates tested in triplicate. PS = polystyrene latex, c/c = capsules per cell.

reported in the [Supporting Information](#)). Moreover, the polyelectrolyte capsules described in this study showed a similar viability pattern to commercial control PS microbeads.

A similar pattern was observed for peripheral blood monocyte, CD4<sup>+</sup> and CD4<sup>-</sup> T cell populations (cf. [Figure 4](#)), as no significant reduction of viability was observed in the cell cultures in the absence of capsules and the inert nontoxic polystyrene latex microspheres.<sup>51</sup> Overall, these results suggest that all four types of polyelectrolyte capsules show a high biocompatibility with hematopoietic cells.

For determination of the uptake/phagocytosis of the non-fluorescent polyelectrolyte capsules by peripheral blood monocytes, in flow cytometry assays, a gating strategy based on the sideward scattering (SSC) characteristics of cells upon phagocytosis was established with size-matched fluorescent beads. Overall, a significant correlation was observed between the two methods of analysis ( $R^2 = 0.934$ ,  $p < 0.01$ ), as similar results were

obtained for both the 5 beads/cell ( $57.0 \pm 0.8\%$  phagocytosis using the method for fluorescent beads ([Figure SI–IV.4.2a](#)) vs  $52.5 \pm 4.5\%$  phagocytosis using the method for nonfluorescent beads ([Figure SI–IV.4.2c](#)) and 10 beads/cell ( $77.3 \pm 2.8\%$  phagocytosis using the method for fluorescent beads ([Figure SI–IV.4.2a](#)) vs  $75.6 \pm 2.6\%$  phagocytosis using the method for non-fluorescent beads ([Figure SI–IV.4.2](#)) conditions (details of all assays are reported in [Supporting Information](#)). The summary shown in [Figure 5](#) indicates that this method can be used for assessment of phagocytosis by monocytes.

Overall, all capsules studied were phagocytosed by monocytes in a dosage-dependent manner, as it was confirmed by previously reported assays. PS microspheres were significantly more efficiently phagocytosed than the polyelectrolyte capsules, even at high capsule per cell ratio (10 particles/cell). No differences were observed in the pattern of uptake for the non-biodegradable PSS/PAH capsules, independently of the charge,

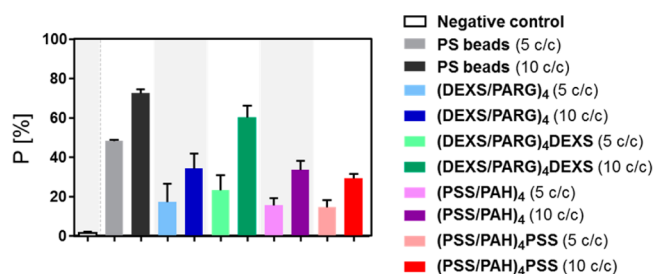


**Figure 5.** Determination of phagocyte microparticles by monocytes, assessed by multiparametric flow cytometry. PBMCs were incubated without (“Negative control”) PS microspheres or polyelectrolyte capsules, during 4 h. Values represent the mean  $\pm$  SD of two biological replicates tested in triplicate.  $P$  [%] = frequency of cells that phagocytosed particles, PS = polystyrene latex,  $c/c$  = capsules per cell.

similarly to the (DEXS/PARG)<sub>4</sub> positively charged biodegradable capsules. In contrast, the negatively charged non-degradable (DEXS/PARG)<sub>4</sub>DEXS capsules at a ratio of 10 capsules/cell were more efficiently phagocytosed than their positively charged counterparts ( $60.4 \pm 5.8\%$  vs  $34.5 \pm 7.5\%$  of cells containing capsules). Considering that the protein corona composition is known to influence the uptake of particles by monocytes and macrophages,<sup>34</sup> and that the charge difference between these beads was associated with a different profile of proteins present in protein corona, it could be speculated that some of the distinct proteins could be facilitating phagocytosis by monocytes. In line with this, the (DEXS/PARG)<sub>4</sub>DEXS displayed complement C3 factor in their protein corona, which was not present in their positively charged counterparts. Considering that bovine and human complement C3 factor share >70% homology (Source: Uniprot), that peripheral blood monocytes express receptors for C3 factor (CR1 and CR3),

and that this opsonin is involved in the recognition and phagocytosis of pathogens, it could be speculated that recognition of the bovine C3 complement factor by monocyte receptors could be involved in the increased uptake of these capsules.

Overall, none of the tested capsules significantly influenced the basal secretion of TNF- $\alpha$  (cf. Figure 6), one of the most ubiquitous and earliest cytokines to be secreted,<sup>52</sup> compared to stimulus with LPS plus IFN $\gamma$ , specifically for the monocytes or PMA plus ionomycin also in T cells. Furthermore, the frequency of TNF- $\alpha$ + cells was systematically lower than the control condition with PS beads, and no association with the degree of cell death and/or phagocytosis was observed. These results suggest that these polyelectrolyte capsules do not elicit an immune response in a short culture (4 h) condition, which would be in line with responses from other immunologically inert materials (e.g., carbon nanotubes<sup>53</sup>). Nevertheless, further studies would be required to assess whether the tested capsules would have an effect with a longer incubation period, or whether they would have the ability to modulate an ongoing immune response, similarly to what has been previously reported for, e.g., carbon nanotubes.<sup>53</sup>

No substantial induction was observed via qPCR. Human PBMCs were incubated with various capsules at 1  $\mu$ g in 200 000 cells in 24 wells for 16 h. LPS was used as a positive control and mock-treated cells as negative control. We found that 16 h is optimum to observe induction of cytokines such as IL-6 and TNF- $\alpha$  in human PBMCs.<sup>54,55</sup> Total RNA was isolated and transformed into cDNA as described. We have not observed any substantial induction in IL-6, which is a general marker for inflammation (cf. Figure 7) or in TNF- $\alpha$  (cf. Figure 8). These mRNA levels are in good agreement with the protein levels observed via flow cytometry.

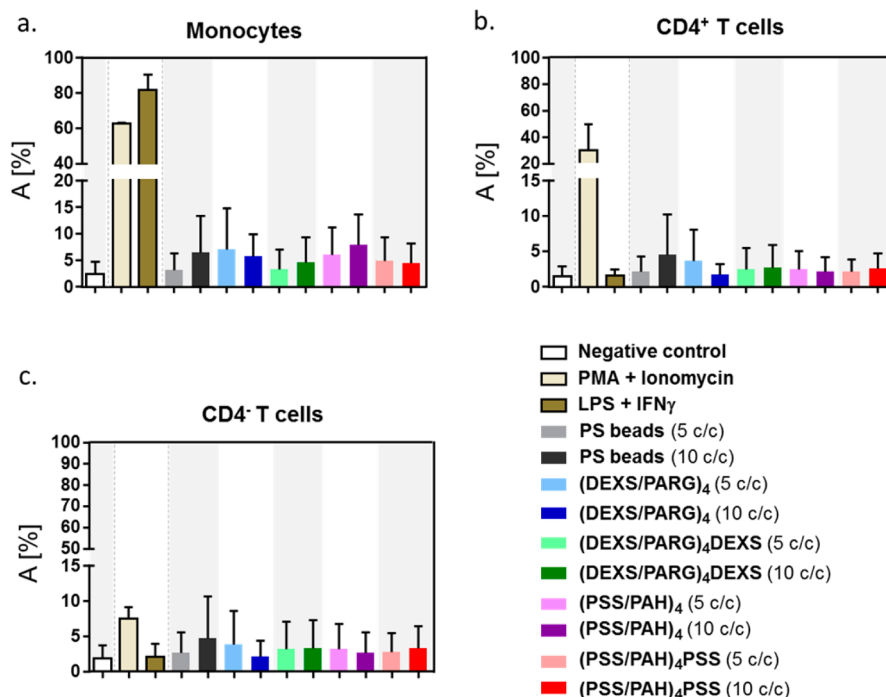


**Figure 6.** Determination of activated cells by phagocyte microparticles, assessed by multiparametric flow cytometry. PBMCs were incubated without (“Negative control”) PS microspheres or polyelectrolyte capsules, during 4 h. Values represent the mean  $\pm$  SD of two biological replicates tested in triplicate.  $A$  [%] = frequency of activated cells that phagocytosed particles, PS = polystyrene latex,  $c/c$  = capsules per cell, LPS = lipopolysaccharide, PMA = phorbol myristate acetate.

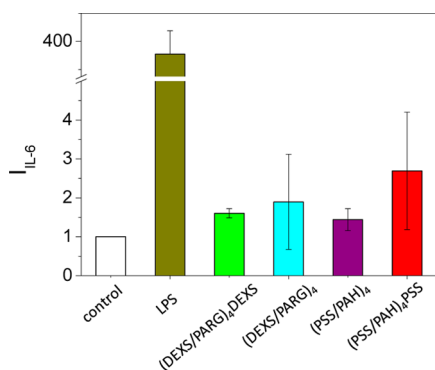


**Figure 7.** IL-6 mRNA levels relative to house keeping genes (mixture) via TagMan. LPS was used as a positive control; control cells are negative (basal level of IL-6) in nontreated PBMCs.

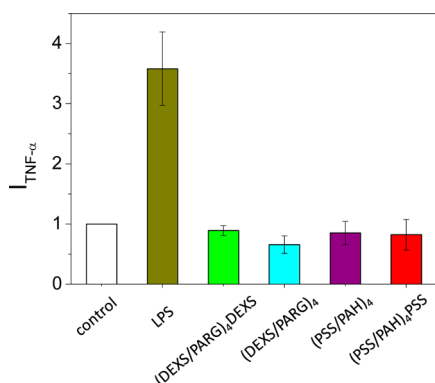


**Figure 8.** TNF- $\alpha$  mRNA levels relative to house keeping genes (mixture) via TagMan. LPS was used as a positive control, Control cells are negative (basal level of TNF- $\alpha$ ) in nontreated PBMCs.

In summary, the tested polyelectrolyte capsules (synthesized by layer-by-layer deposition) are biocompatible, because the uptake of capsules did not increase the expression of TNF- $\alpha$  and IL-6, among others, in peripheral blood mononuclear cells, in comparison with conventional antigen stimulus. As another additional property, these capsules are easily taken up at relevant concentration for practical applications in several different cell lines. With these obtained results in mind, the tested polyelectrolyte capsules should be suitable for bioapplications in complex biological samples due to easily tested uptake and immunocompatibility.

## EXPERIMENTAL PROCEDURES

**Synthesis and Characterization of Polyelectrolyte Capsules.** Four different types of capsules were synthesized using  $\text{CaCO}_3$  template cores:<sup>56</sup> (i) positively charged degradable dextran sulfate/poly(L-arginine) capsules  $(\text{DEXS/PARG})_4$  (4 refers to the number of bilayers), (ii) negatively charged degradable dextran sulfate/poly(L-arginine) capsules  $(\text{DEXS/PARG})_4\text{DEXS}$ , (iii) positively charged non-degradable poly(sodium 4-styrenesulfonate)/poly(allylamine hydrochloride) capsules  $(\text{PSS/PAH})_4$ , and (iv) negatively charged non-degradable poly(sodium 4-styrenesulfonate)/poly(allylamine hydrochloride) capsules  $(\text{PSS/PAH})_4\text{PSS}$ . Sketch of capsules are shown in Figure 1. To monitor the internalization of capsules dextran labeled with the pH sensitive fluorescent dye seminaphtharhodafuor (SNARF-1) was optionally integrated in the cavity of the capsules, according to previously published protocols.<sup>33,44</sup>

The emission of SNARF-1 shifts from 580 nm in acidic media to 640 nm in alkaline media. Capsules were characterized by optical microscopy and transmission electron microscopy. Details and the full data set are given in the Supporting Information.

**Protein Corona Formation.** Capsules were incubated in cell culture medium supplemented with 10% fetal bovine serum (FBS). After several rinsing steps the proteins adherent to the capsules were quantified by tandem mass spectrometry, according to previously reported protocols.<sup>57</sup> More detailed information is reported in the Supporting Information.

**Quantification of the Capsule Uptake by Different Cell Lines.** The human lung adenocarcinoma cell line A549, the human cervical carcinoma cell line HeLa, and human monocyte-derived macrophages (HMDM) as primary cells<sup>58</sup> were incubated with 5 or 10 capsules (in the case of capsules containing SNARF-1) added per cell for 12 or 24 h in cell medium supplemented with 10% serum. Then cells were imaged by fluorescence microscopy, and at least for 50 different cells for each sample the number of internalized capsules  $N$  was counted, as reported already in previous studies.<sup>31,32,59</sup> The color of emission of SNARF-1 allowed for distinguishing between internalized capsules (acidic environment) and capsules only adherent to the outer cell membrane (neutral/slightly alkaline environment).<sup>33,60,61</sup> As a result a histogram of the frequency  $f(N)$  that a cell has internalized  $N$  capsules could be plotted for each sample and incubation condition.  $f(N)$  is normalized as  $\sum_{i=0}^{\infty} f(i) = 1$ . From the  $f(N)$  data the cumulative distribution functions  $p(N) = \sum_{i=0}^N f(i)$  were calculated, which describe the probability that a cell contains  $N$  or fewer internalized capsules.<sup>28,32</sup>

**Immunocompatibility of the Capsules Was Assessed by Flow Cytometry.** Several flow cytometry assays were finally combined in order to determine, simultaneously, cell death (SI IV.6), phagocytosis (SI IV.4), and cytokine production (SI IV.7) caused by the different capsules. This phagocytosis–cell activation–cell death (PAD) assay has been described in Patent EP16382317.2.<sup>62</sup> Polystyrene latex (PS) beads were used as a control. Immunophenotypic studies were performed on PBMCs isolated from whole peripheral blood of two healthy volunteers (SI IV.3). A total of 200 000 PBMCs were cultured in RPMI-1640 medium supplemented with 10% FBS and 40  $\mu\text{M}$  TACE inhibitor in a 24-well plate, and they were incubated with 5 and 10 capsules added per cell for 4 h. Cells stimulated with PMA (10 ng/mL) plus ionomycin (0.75  $\mu\text{g}/\text{mL}$ ) or LPS (100 ng/mL) plus IFN $\gamma$  (10 ng/mL) were used as positive controls of TNF- $\alpha$  production in peripheral blood T-cells and monocytes, respectively. Furthermore, TACE inhibitor and brefeldin A (10  $\mu\text{g}/\text{mL}$ ) were used as secretion blocking agents to reveal the levels of surface versus surface plus cytoplasmic expression of TNF- $\alpha$ . After the incubation period, cells were detached with a cell scraper and collected by centrifugation. These cells were systematically stained with the annexin-V pacific blue (PacB) (ImmunoStep, Salamanca)/CD4 phycoerythrin (PE) (ImmunoStep, Salamanca. Clone HP2/6)/CD45 peridinin chlorophyll protein (PerCP)-cyanin 5.5 (Cy5.5) (Becton Dickinson Biosciences, BD, San Jose/CA, USA. Clone 2D1)/CD14 PE-cyanin 7 (Cy7) (BD, San Jose/CA, USA. Clone RM052)/ TNF- $\alpha$  allophycocyanin (APC) (BD, San Jose/CA, USA. Clone Mab11)/CD3 APC-H7 (BD, San Jose/CA, USA. Clone SK7) combination of monoclonal antibodies (MoAb) for 15 min at room temperature. Data acquisition was performed in a FACSCanto II flow cytometer (Becton Dickinson Biosciences, BD, San Jose/CA, USA) using

the FACSDiva software (v 6.1, BD). For data analysis, the Infinicyt software (Cytognos SL, Salamanca, Spain) was used. Data analysis was performed in five steps. First, we selected the cells of interest (white blood cells) and excluded cell debris and cell aggregates, based on the expression of CD45 and light dispersion characteristics (forward side scatter (FSC) and side-ward side scatter (SSC)). Second, we identified and selected the monocytes (CD14<sup>++</sup>/CD4<sup>+</sup>/CD3<sup>-</sup>/CD45<sup>+</sup>), the T-CD4<sup>+</sup> lymphocytes (CD45<sup>++</sup>/CD3<sup>+</sup>/CD4<sup>+</sup>/CD14<sup>-</sup>), and the T-CD4<sup>-</sup> lymphocytes (CD45<sup>++</sup>/CD3<sup>+</sup>/CD4<sup>-</sup>/CD14<sup>-</sup>) (cf. Figure SI–IV.5.1). Third, we selected Annexin V-CFBlue positive cells within each population corresponding to apoptotic cells (cf. Figure SI–IV.6.1). Afterward, non-annexin positive cells (corresponding to viable cells) were used for determining TNF- $\alpha$ -APC positive cells (for measuring the immune response) (cf. Figure SI–IV.7.1). The effect of the stimulation in each cell population was assessed on unstimulated samples as a control, and TNF- $\alpha$  production was based on the percentage of positive cells, after subtracting the percentage of cells staining above the threshold for positivity in the negative control. Finally, phagocytic cells were identified selecting positive cells in the FITC channel (cf. Figure SI–IV.8.1) or, for the nonfluorescent capsules, selected based on FSC and SSC features (cf. Figure SI–IV.4.2). A detailed description of materials and methods and validation of the strategy for phagocytosis assessment are given in the Supporting Information.

**Immunocompatibility of the Capsules Assessed by Real-Time Polymerase Chain Reaction (qPCR) Analysis in Human Peripheral Mononuclear Cells (PBMC).** PBMCs were obtained from healthy donors from Rabin Medical Center (Petah Tikva, Israel) after obtaining institutional review board-approved informed consent. To isolate low-density cells, PBMCs were fractionated using Ficoll-Paque PLUS (GE Healthcare, Life Sciences). Fractionated cells were used immediately. PBMCs cells (60% confluence, 200 000 cells) in 24-well dishes were treated with 1  $\mu$ g of each different type of capsules for 16 h. Total RNA was isolated using EZ-RNA kit (Biological Industries, Israel) and cDNA was generated with a high capacity cDNA kit (Life Technologies, Carlsbad, CA, USA) according to the manufacturers' protocols. QPCR was performed with TagMan of IL-6 and TNF- $\alpha$  on the ABI StepOnePlus instrument (Life Technologies, Carlsbad, CA, USA).

## ■ ASSOCIATED CONTENT

### ● Supporting Information

The Supporting Information is available free of charge on the ACS Publications website at DOI: 10.1021/acs.bioconjchem.6b00657.

Detailed description of experimental procedures and evaluation protocols (PDF)

## ■ AUTHOR INFORMATION

### Corresponding Authors

\*E-mail: peer@tauex.tau.ac.il.

\*E-mail: mfuentes@usal.es.

\*E-mail: wolfgang.parak@physik.uni-marburg.de.

### ORCID

Alberto Escudero: 0000-0002-0850-6589

Wolfgang J. Parak: 0000-0003-1672-6650

### Notes

The authors declare no competing financial interest.

## ■ ACKNOWLEDGMENTS

This work was supported by the German Research Foundation (DFG grant PA 794/21-1 to W.J.P.) and the Sino-German cooperative project No. GZ 905 from the Sino German Center. We gratefully acknowledge financial support from the Carlos III Health Institute of Spain (ISCIII, FIS PI14/01538), Fondos FEDER (EU), Junta Castilla-León BIO/SA07/15, Fundación Solórzano FS/23-2015. The Proteomics Units belongs to ProteoRed, PRB2-ISCIII, supported by grant PT13/0001. P.D. is supported by a JCYL-EDU/346/2013 PhD scholarship. D.P. acknowledges the FTA: Nanomedicines for Personalized Theranostics of the Israeli National Nanotechnology Initiative and the Leona M. and Harry B. Helmsley Nanotechnology Research Fund. A.E. acknowledges Junta de Andalucía (Spain) for a Talenta Postdoc Fellowship, cofinanced by the European Union Seventh Framework Programme, grant agreement no 267226.

## ■ REFERENCES

- (1) Donath, E., Sukhorukov, G. B., Caruso, F., Davis, S. A., and Möhwald, H. (1998) Novel hollow Polymer shells by colloid-templated assembly of polyelectrolytes. *Angew. Chem., Int. Ed.* 37, 2201–2205.
- (2) Sukhorukov, G. B., Donath, E., Davis, S., Lichtenfeld, H., Caruso, F., Popov, V. I., and Möhwald, H. (1998) Stepwise polyelectrolyte assembly on particle surfaces: a novel approach to colloid design. *Polym. Adv. Technol.* 9, 759–767.
- (3) De Koker, S., De Cock, L. J., Rivera-Gil, P., Parak, W. J., Veltj, R. A., Vervaet, C., Remon, J. P., Grooten, J., and De Geest, B. G. (2011) Polymeric multilayer capsules delivering biotherapeutics. *Adv. Drug Delivery Rev.* 63, 748–761.
- (4) Hussain, S. Z., Zyuzin, M. V., Hussain, I., Parak, W. J., and Carregal-Romero, S. (2016) Catalysis by multifunctional polyelectrolyte capsules. *RSC Adv.* 6, 81569–81577.
- (5) Sukhorukov, G. B., Rogach, A. L., Garstka, M., Springer, S., Parak, W. J., Muñoz-Javier, A., Kreft, O., Skirtach, A. G., Susha, A. S., Ramaye, Y., Palankar, R., and Winterhalter, M. (2007) Multifunctionalized polymer microcapsules: novel tools for biological and pharmacological applications. *Small* 3, 944–955.
- (6) Rivera Gil, P., del Mercato, L. L., del Pino, P., Muñoz-Javier, A., and Parak, W. J. (2008) Nanoparticle-modified polyelectrolyte capsules. *Nano Today* 3, 12–21.
- (7) Xiao, F. X., Pagliaro, M., Xu, Y. J., and Liu, B. (2016) Layer-by-layer assembly of versatile nanoarchitectures with diverse dimensionality: a new perspective for rational construction of multilayer assemblies. *Chem. Soc. Rev.* 45, 3088–3121.
- (8) del Mercato, L. L., Ferraro, M. M., Baldassarre, F., Mancarella, S., Greco, V., Rinaldi, R., and Leporatti, S. (2014) Biological applications of LbL multilayer capsules: From drug delivery to sensing. *Adv. Colloid Interface Sci.* 207, 139–154.
- (9) Muñoz Javier, A., del Pino, P., Bedard, M. F., Skirtach, A. G., Ho, D., Sukhorukov, G. B., Plank, C., and Parak, W. J. (2008) Photoactivated release of cargo from the cavity of polyelectrolyte capsules to the cytosol of cells. *Langmuir* 24, 12517–12520.
- (10) del Mercato, L. L., Abbasi, A. Z., Ochs, M., and Parak, W. J. (2011) Multiplexed sensing of ions with barcoded polyelectrolyte capsules. *ACS Nano* 5, 9668–9674.
- (11) Richardson, J. J., Björnmalm, M., and Caruso, F. (2015) Technology-driven layer-by-layer assembly of nanofilms. *Science* 348, 6233.
- (12) De Koker, S., De Geest, B. G., Cuvelier, C., Ferdinande, L., Deckers, W., Hennink, W. E., De Smedt, S., and Mertens, N. (2007) In vivo cellular uptake, degradation, and biocompatibility of polyelectrolyte microcapsules. *Adv. Funct. Mater.* 17, 3754–3763.
- (13) Gnanadhas, D. P., Ben Thomas, M., Elango, M., Raichur, A. M., and Chakravorty, D. (2013) Chitosan-dextran sulphate nanocapsule drug delivery system as an effective therapeutic against intra-

phagosomal pathogen Salmonella. *J. Antimicrob. Chemother.* 68, 2576–2586.

(14) Moskowitz, J. S., Blaisse, M. R., Samuel, R. E., Hsu, H.-P., Harris, M. B., Martin, S. D., Lee, J. C., Spector, M., and Hammond, P. T. (2010) The effectiveness of the controlled release of gentamicin from polyelectrolyte multilayers in the treatment of Staphylococcus aureus infection in a rabbit bone model. *Biomaterials* 31, 6019–6030.

(15) De Geest, B. G., Willart, M. A., Hammad, H., Lambrecht, B. N., Pollard, C., Bogaert, P., De Filette, M., Saelens, X., Vervaet, C., Remon, J. P., Grooten, J., and De Koker, S. (2012) Polymeric multilayer capsule-mediated vaccination induces protective immunity against cancer and viral infection. *ACS Nano* 6, 2136–2149.

(16) De Koker, S., Naessens, T., De Geest, B. G., Bogaert, P., Demeester, J., De Smedt, S., and Grooten, J. (2010) Biodegradable polyelectrolyte microcapsules: antigen delivery tools with Th17 skewing activity after pulmonary delivery. *J. Immunol.* 184, 203–211.

(17) Sexton, A., Whitney, P. G., Chong, S.-F., Zelikin, A. N., Johnston, A. P. R., De Rose, R., Brooks, A. G., Caruso, F., and Kent, S. J. (2009) A protective vaccine delivery system for in vivo T cell stimulation using nanoengineered polymer hydrogel capsules. *ACS Nano* 3 (11), 3391–3400.

(18) Facca, S., Cortez, C., Mendoza-Palomares, C., Messadeq, N., Dierich, A., Johnston, A. P., Mainard, D., Voegel, J. C., Caruso, F., and Benkirane-Jessel, N. (2010) Active multilayered capsules for in vivo bone formation. *Proc. Natl. Acad. Sci. U. S. A.* 107, 3406–11.

(19) Peng, L. H., Zhang, Y. H., Han, L. J., Zhang, C. Z., Wu, J. H., Wang, X. R., Gao, J. Q., and Mao, Z. W. (2015) Cell membrane capsules for encapsulation of chemotherapeutic and cancer cell targeting in vivo. *ACS Appl. Mater. Interfaces* 7, 18628–18637.

(20) Richardson, J. J., Choy, M. Y., Guo, J., Liang, K., Alt, K., Ping, Y., Cui, J., Law, L. S., Hagemeyer, C. E., and Caruso, F. (2016) Polymer capsules for plaque-targeted in vivo delivery. *Adv. Mater.* 28, 7703–7707.

(21) Shao, J. X., Xuan, M. J., Si, T. Y., Dai, L. R., and He, Q. (2015) Biointerfacing polymeric microcapsules for in vivo near-infrared light-triggered drug release. *Nanoscale* 7, 19092–19098.

(22) Ambrosone, A., Marchesano, V., Carregal-Romero, S., Intartaglia, D., Parak, W. J., and Tortiglione, C. (2016) Control of wnt/ $\beta$ -catenin signaling pathway in vivo via light responsive capsules. *ACS Nano* 10, 4828–4834.

(23) Shao, J. X., Xuan, M. J., Dai, L. R., Si, T. Y., Li, J. B., and He, Q. (2015) Near-infrared-activated nanocalorifiers in microcapsules: vapor bubble generation for in vivo enhanced cancer therapy. *Angew. Chem., Int. Ed.* 54, 12782–12787.

(24) Chen, H. Y., Di, Y. F., Chen, D., Madrid, K., Zhang, M., Tian, C. P., Tang, L. P., and Gu, Y. Q. (2015) Combined chemo- and photothermal therapy delivered by multifunctional theranostic gold nanorod-loaded microcapsules. *Nanoscale* 7, 8884–8897.

(25) Yi, Q., Li, D., Lin, B., Pavlov, A. M., Luo, D., Gong, Q., Song, B., and Ai, H. (2014) Magnetic resonance imaging for monitoring of magnetic polyelectrolyte capsule in vivo delivery. *Bionanosci.* 4, 59–70.

(26) De Geest, B. G., Willart, M. A., Lambrecht, B. N., Pollard, C., Vervaet, C., Remon, J. P., Grooten, J., and De Koker, S. (2012) Surface-engineered polyelectrolyte multilayer capsules-synthetic vaccines mimicking microbial structure and function. *Angew. Chem., Int. Ed.* 51, 3862–3866.

(27) Kuhn, D. A., Hartmann, R., Fytianos, K., Petri-Fink, A., Rothen-Rutishauser, B., and Parak, W. J. (2015) Cellular uptake and cell-to-cell transfer of polyelectrolyte microcapsules within a triple co-culture system representing parts of the respiratory tract. *Sci. Technol. Adv. Mater.* 16, 034608.

(28) Kastl, L., Sasse, D., Wulf, V., Hartmann, R., Mircheski, J., Ranke, C., Carregal-Romero, S., Martínez-López, J. A., Fernández-Chacón, R., Parak, W. J., Elsasser, H. P., and Rivera-Gil, P. (2013) Multiple internalization pathways of polyelectrolyte multilayer capsules into mammalian cells. *ACS Nano* 7, 6605–6618.

(29) Muñoz Javier, A., Kreft, O., Semmling, M., Kempter, S., Skirtach, A. G., Bruns, O., del Pino, P., Bedard, M. F., Rädler, J., Käs, J., Plank, C., Sukhorukov, G. B., and Parak, W. J. (2008) Uptake of colloidal

polyelectrolyte coated particles and polyelectrolyte multilayer capsules by living cells. *Adv. Mater.* 20, 4281–4287.

(30) Rivera-Gil, P., de Koker, S., De Geest, B. G., and Parak, W. J. (2009) Intracellular processing of proteins mediated by biodegradable polyelectrolyte capsules. *Nano Lett.* 9 (12), 4398–4402.

(31) Muñoz Javier, A., Kreft, O., Piera Alberola, A., Kirchner, C., Zebli, B., Susha, A. S., Horn, E., Kempter, S., Skirtach, A. G., Rogach, A. L., Rädler, J., Sukhorukov, G. B., Benoit, M., and Parak, W. J. (2006) Combined atomic force microscopy and optical microscopy measurements as a method to investigate particle uptake by cells. *Small* 2, 394–400.

(32) Parakhonskiy, B., Zyuzin, M. V., Yashchenok, A., Carregal-Romero, S., Rejman, J., Mohwald, H., Parak, W. J., and Skirtach, A. G. (2015) The influence of the size and aspect ratio of anisotropic, porous CaCO<sub>3</sub> particles on their uptake by cells. *J. Nanobiotechnol.* 13, 53.

(33) Hartmann, R., Weidenbach, M., Neubauer, M., Fery, A., and Parak, W. J. (2015) Stiffness-dependent in vitro uptake and lysosomal acidification of colloidal particles. *Angew. Chem., Int. Ed.* 54, 1365–1368.

(34) Yan, Y., Gause, K. T., Kamphuis, M. M. J., Ang, C.-S., O'Brien-Simpson, N. M., Lenzo, J. C., Reynolds, E. C., Nice, E. C., and Caruso, F. (2013) Differential roles of the protein corona in the cellular uptake of nanoporous polymer particles by monocyte and macrophage cell lines. *ACS Nano* 7, 10960–10970.

(35) Kirchner, C., Javier, A. M., Susha, A. S., Rogach, A. L., Kreft, O., Sukhorukov, G. B., and Parak, W. J. (2005) Cytotoxicity of nanoparticle-loaded polymer capsules. *Talanta* 67, 486–491.

(36) Shi, D. J., Ran, M. S., Zhang, L., Huang, H., Li, X. J., Chen, M. Q., and Akashi, M. (2016) Fabrication of biobased polyelectrolyte capsules and their application for glucose-triggered insulin delivery. *ACS Appl. Mater. Interfaces* 8, 13688–13697.

(37) Lomova, M. V., Brichkina, A. I., Kiryukhin, M. V., Vasina, E. N., Pavlov, A. M., Gorin, D. A., Sukhorukov, G. B., and Antipina, M. N. (2015) Multilayer capsules of bovine serum albumin and tannic acid for controlled release by enzymatic degradation. *ACS Appl. Mater. Interfaces* 7, 11732–11740.

(38) Lukaszewicz, S., and Szczepanowicz, K. (2014) In Vitro Interaction of polyelectrolyte nanocapsules with model Cells. *Langmuir* 30, 1100–1107.

(39) Gao, H., Wen, D. S., Tarakina, N. V., Liang, J. R., Bushby, A. J., and Sukhorukov, G. B. (2016) Bifunctional ultraviolet/ultrasound responsive composite TiO<sub>2</sub>/polyelectrolyte microcapsules. *Nanoscale* 8, 5170–5180.

(40) del Mercato, L. L., Guerra, F., Lazzari, G., Nobile, C., Bucci, C., and Rinaldi, R. (2016) Biocompatible multilayer capsules engineered with a graphene oxide derivative: synthesis, characterization and cellular uptake. *Nanoscale* 8, 7501–7512.

(41) Wang, B., Zhang, Y., Mao, Z., and Gao, C. (2012) Cellular uptake of covalent poly(allylamine hydrochloride) microcapsules and its influences on cell functions. *Macromol. Biosci.* 12, 1534–45.

(42) Ganas, C., Weiß, A., Nazarenus, M., Rösler, S., Kissel, T., Rivera-Gil, P., and Parak, W. J. (2014) Biodegradable capsules as non-viral vectors for in vitro delivery of PEI/siRNA polyplexes for efficient gene silencing. *J. Controlled Release* 196, 132–138.

(43) Zelikin, A. N., Breheney, K., Robert, R., Tjijto, E., and Wark, K. (2010) Cytotoxicity and internalization of polymer hydrogel capsules by mammalian cells. *Biomacromolecules* 11, 2123–2129.

(44) Ott, A., Yu, X., Hartmann, R., Rejman, J., Schütz, A., Ochs, M., Parak, W. J., and Carregal-Romero, S. (2015) Light-addressable and degradable silica capsules for delivery of molecular cargo to the cytosol of cells. *Chem. Mater.* 27, 1929–1942.

(45) Gao, H., Goriacheva, O. A., Tarakina, N. V., and Sukhorukov, G. B. (2016) Intracellularly biodegradable polyelectrolyte/silica composite microcapsules as carriers for small Molecules. *ACS Appl. Mater. Interfaces* 8, 9651–9661.

(46) Kolbe, A., del Mercato, L. L., Abbasi, A. Z., Rivera-Gil, P., Gorzini, S. J., Huibers, W. H. C., Poolman, B., Parak, W. J., and Herrmann, A. (2011) De Novo design of supercharged, unfolded

protein polymers, and their assembly into supramolecular aggregates. *Macromol. Rapid Commun.* 32, 186–190.

(47) Dierendonck, M., De Koker, S., Vervaet, C., Remon, J. P., and De Geest, B. G. (2012) Interaction between polymeric multilayer capsules and immune cells. *J. Controlled Release* 161, 592–599.

(48) Kreft, O., Muñoz Javier, A., Sukhorukov, G. B., and Parak, W. J. (2007) Polymer microcapsules as mobile local pH-sensors. *J. Mater. Chem.* 17, 4471–4476.

(49) Jahnhen-Dechent, W., Schafer, C., Ketteler, M., and McKee, M. D. (2008) Mineral chaperones: a role for fetuin-A and osteopontin in the inhibition and regression of pathologic calcification. *J. Mol. Med. (Heidelberg, Ger.)* 86, 379–389.

(50) Heiss, A., Eckert, T., Aretz, A., Richtering, W., Van Dorp, W., Schafer, C., and Jahnhen-Dechent, W. (2008) Hierarchical role of fetuin-A and acidic serum proteins in the formation and stabilization of calcium phosphate particles. *J. Biol. Chem.* 283, 14815–14825.

(51) Karlson, T. D., Kong, Y. Y., Hardy, C. L., Xiang, S. D., and Plebanski, M. (2013) The signalling imprints of nanoparticle uptake by bone marrow derived dendritic cells. *Methods* 60, 275–283.

(52) Mascher, B., Schlenke, P., and Seyfarth, N. (1999) Expression and kinetics of cytokines determined by intracellular staining using flow cytometry. *J. Immunol. Methods* 223, 115–121.

(53) Laverny, G., Casset, A., Purohit, A., Schaeffer, E., Spiegelhalter, C., de Blay, F., and Pons, F. (2013) Immunomodulatory properties of multi-walled carbon nanotubes in peripheral blood mononuclear cells from healthy subjects and allergic patients. *Toxicol. Lett.* 217, 91–101.

(54) Landesman-Milo, D., and Peer, D. (2014) Toxicity profiling of several common RNAi-based nanomedicines: a comparative study. *Drug Delivery Transl. Res.* 4, 96–103.

(55) Peer, D., Zhu, P. C., Carman, C. V., Lieberman, J., and Shimaoka, M. (2007) Selective gene silencing in activated leukocytes by targeting siRNAs to the integrin lymphocyte function-associated antigen-1. *Proc. Natl. Acad. Sci. U. S. A.* 104, 4095–4100.

(56) Wang, Y., Moo, Y. X., Chen, C., Gunawan, P., and Xu, R. (2010) Fast precipitation of uniform CaCO<sub>3</sub> nanospheres and their transformation to hollow hydroxyapatite nanospheres. *J. Colloid Interface Sci.* 352, 393–400.

(57) Mahmoudi, M., Abdelmonem, A. M., Behzadi, S., Clement, J. H., Dutz, S., Ejtehadi, M. R., Hartmann, R., Kantner, K., Linne, U., Maffre, P., Metzler, S., Moghadam, M. K., Pfeiffer, C., Rezaei, M., Ruiz-Lozano, P., Serpooshan, V., Shokrgozar, M. A., Nienhaus, G. U., and Parak, W. J. (2013) Temperature: the "ignored" factor at the nanobio interface. *ACS Nano* 7, 6555–6562.

(58) Blank, F., Wehrli, M., Lehmann, A., Baum, O., Gehr, P., von Garnier, C., and Rothen-Rutishauser, B. M. (2011) Macrophages and dendritic cells express tight junction proteins and exchange particles in an in vitro model of the human airway wall. *Immunobiology* 216, 86–95.

(59) Sukhorukov, G. B., Rogach, A. L., Zebli, B., Liedl, T., Skirtach, A. G., Köhler, K., Antipov, A. A., Gaponik, N., Susha, A. S., Winterhalter, M., and Parak, W. J. (2005) Nanoengineered polymer capsules: Tools for detection, controlled delivery and site specific manipulation. *Small* 1, 194–200.

(60) Semmling, M., Kreft, O., Muñoz Javier, A., Sukhorukov, G. B., Käs, J., and Parak, W. J. (2008) A novel flow-cytometry-based assay for cellular uptake studies of polyelectrolyte microcapsules. *Small* 4, 1763–1768.

(61) Feliu, N., Hühn, J., Zyuzin, M. V., Ashraf, S., Valdeperez, D., Masood, A., Said, A. H., Escudero, A., Pelaz, B., Gonzalez, E., Duarte, M. A., Roy, S., Chakraborty, I., Lim, M. L., Sjöqvist, S., Jungebluth, P., and Parak, W. J. (2016) Quantitative uptake of colloidal particles by cell cultures. *Sci. Total Environ.* 568, 819–828.

(62) Fuentes, G. M., Garcia, M. P. D., Teodosio, C. I. G. G., Matos, A. O. D., and Acevedo, R. J. (2016) One step phagocytosis-cell activation-cell death assay. European Patent No. EP16382317.